Pakistan Veterinary Journal

ISSN: 0253-8318 (PRINT), 2074-7764 (ONLINE)
DOI: 10.29261/pakvetj/2025.295

RESEARCH ARTICLE

# DOCK2 Deficiency Alleviates Murine Spinal Cord Ischemia-Reperfusion Injury via Inhibiting Autophagy-Dependent Ferroptosis and the Modulatory Role of Sevoflurane Pretreatment

Huijun Liu[1#], Yu Li[1#], Junya Li[2], Tengfei Wu[3], Jinpeng Liu[4], Hongnan Wang[1*] and Jie Han[1*]

[1]Department of Anesthesiology, The First Affiliated Hospital of China Medical University, Shenyang, China; [2]Fourth Clinical College, China Medical University, Shenyang, China; [3]Department of Laboratory Animal Science, China Medical University, Shenyang, China; [4]College of Animal Science and Veterinary Medicine, Shenyang Agricultural University, Shenyang, China

[#] These authors contributed to the work equally and should be regarded as co-first authors.
*Corresponding author: whn458526733647@163.com (HW); hj077231@hotmail.com (JH)

ARTICLE HISTORY (25-893)

Received: September 14, 2025
Revised: October 29, 2025
Accepted: November 01, 2025
Published online: November 13, 2025

**Key words:**
Autophagy
DOCK2
Ferroptosis
Sevoflurane
Spinal cord ischemia-reperfusion injury

**ABSTRACT**

Spinal cord ischemia-reperfusion injury (SCIRI) is a serious complication in veterinary practice, particularly following aortic cross-clamping during equine colic surgery, with no proven therapies for its neurological sequelae. Autophagy and ferroptosis drive SCIRI pathogenesis, but DOCK2's role remains unclear. We investigated DOCK2 using 110 male C57BL/6 wild-type (WT, n=6/group) and 6 DOCK2-deficient (DOCK2-KO) mice and oxygen-glucose deprivation/reoxygenation (OGD/R)-treated primary spinal neurons. Murine SCIRI was induced by clamping the abdominal aorta and spinal cord DOCK2 expression was increased post SCIRI, peaking at 24 h. DOCK2 deficiency also enhanced viability by 40% of primary spinal neurons under oxygen-glucose deprivation/reoxygenation (OGD/R) conditions. SCIRI mice exhibited improved motor function recovery, reduced spinal cord pathological damage following DOCK2 knockdown. Mechanistically, we revealed that DOCK2 deficiency suppressed excessive ferroptosis-mediated by autophagy *in vivo* and *in vitro*. Notably, the protective effects of DOCK2 deficiency were abolished by autophagy activator rapamycin. Moreover, sevoflurane pretreatment exerted a protective effect against SCIRI, which was abrogated by DOCK2 overexpression. In conclusion, DOCK2 mediates SCIRI via autophagy-dependent ferroptosis and is a potential therapeutic target. Sevoflurane protects against SCIRI by inhibiting DOCK2, providing a basis for perioperative SCIRI management in animals.

**To Cite This Article:** Huijun Liu, Yu Li, Junya Li, Tengfei Wu, Jinpeng Liu, Hongnan Wang and Jie Han, 2025. DOCK2 deficiency alleviates murine spinal cord ischemia-reperfusion injury via inhibiting autophagy-dependent ferroptosis and the modulatory role of sevoflurane pretreatment. Pak Vet J. http://dx.doi.org/10.29261/pakvetj/2025.295

## INTRODUCTION

Spinal cord ischemia-reperfusion injury (SCIRI) constitutes a critical complication in veterinary practice, particularly following spinal surgery, aortic occlusion, or traumatic injury in companion animals and livestock (Hafezi *et al.*, 2024). The pathophysiological cascade of SCIRI is characterized by an initial ischemic insult resulting in critical hypoperfusion/infarct of spinal cord tissue, followed by the reestablishment of blood flow (Hu *et al.*, 2016; Lin *et al.*, 2021). Paradoxically, the reperfusion phase can amplify the initial ischemic damage through a series of mechanisms, including robust inflammatory activation, oxidative stress, mitochondrial dysfunction, and cellular apoptosis, ultimately leading to extended secondary injury (Borgens and Liu-Snyder, 2012; Xing *et al.*, 2025). Pathologically, SCIRI involves a cascade of biological process that culminate in neuronal death and motor dysfunction. To mitigate the risk of SCIRI, various strategies have been explored, including pharmacological preconditioning (Azari *et al.*, 2015; Bell *et al.*, 2012; Eryilmaz and Farooque, 2021). Numerous pharmacological agents, such as steroids, free-radical scavengers, and vasodilators, have shown efficacy in preclinical models of SCIRI (Awad *et al.*, 2021; Simon *et al.*, 2019), however, their translational success remains limited and no therapy has proven fully effective in preventing SCIRI in clinical settings.

It is well accepted that autophagy and ferroptosis represent two programmed neuronal death cellular processes and are increasingly recognized as key regulators of

neurological injury pathogenesis (Shi *et al.*, 2021; Zhu *et al.*, 2024). Autophagy, a conserved catabolic pathway, maintains homeostasis by clearing damaged organelles, but its dysregulation can be found during SCIRI (Wang *et al.*, 2010; Zhou *et al.*, 2017). Autophagy is typically maintained at a basal level under physiological conditions, while its activity can be significantly upregulated in response to pathological stimulation, such as ischemia, hypoxia, or nutrient deprivation (Liu *et al.*, 2023; Mizushima and Komatsu, 2011). The previous studies have demonstrated that SCIRI upregulates the expression of key autophagy markers, including microtubule-associated protein 1 light chain 3 (LC3) and Beclin-1 (Yin *et al.*, 2019). Although the physiological levels of autophagy contribute to maintain intracellular homeostasis and promote cell survival, excessive autophagic activation can ultimately lead to autophagic cell death (Luo and Tao, 2020; Xu and Li, 2020). Emerging evidence indicates the complicated crosstalk is tightly intertwined with SCIRI pathogenesis, as dysregulated autophagy can either promote or inhibit ferroptosis depending on the stage and severity of spinal cord ischemic injury. Ferroptosis, an iron-dependent form of regulated cell death driven by lipid peroxidation, has been implicated in a broad spectrum of pathological conditions, including cancer, neurodegenerative disorders, acute kidney injury and spinal cord injury progression (Stockwell *et al.*, 2020; Zheng *et al.*, 2025). Besides, the protective effects of deferoxamine, an inhibitor of ferroptosis, showing improved hindlimb function and reduced neuronal loss in rat models (Yao *et al.*, 2019). Specifically, autophagic clearance of iron-containing organelles or lipid peroxidation products may modulate ferroptosis sensitivity, while ferroptotic signals can in turn feedback to regulate autophagic flux in injured neurons. In veterinary medicine, emerging evidence has suggested that autophagy–ferroptosis crosstalk significantly contributes to the pathogenesis of SCIRI. Thus, targeted exploration of novel drugs targeting autophagy and ferroptosis in SCIRI is essential.

Dedicator of cytokinesis 2 (DOCK2), a Rac1 GTPase activator, has recently emerged as a potential regulator of neurological disorders beyond its established role in immune cell function (Ji *et al.*, 2022). The recent studies have indicated that DOCK2 involves in various biological processes (Guo and Chen, 2017; Sabzvar *et al.*, 2025). Furthermore, DOCK2 ablation modulates microglial innate immune responses, thereby influencing amyloid-beta plaque burden in Alzheimer's disease (Cimino *et al.*, 2013). Recent studies suggested that downregulation of DOCK2 conferred protection against cerebral ischemia reperfusion injury by promoting microglial polarization toward a protective M2 phenotype through regulation of the STAT6 signaling pathway (Ding *et al.*, 2022). Given the conserved function of DOCK2, we hypothesize that DOCK2-mediated autophagic flux dysregulation promotes ferroptosis during SCIRI. This study aims to investigate DOCK2 expression dynamics in murine SCIRI models and primary neurons subjected to oxygen-glucose deprivation/reoxygenation, and to elucidate its role as a therapeutic target for improving veterinary SCIRI outcomes.

## MATERIALS AND METHODS

**Experimental Animals and Ethical Approval:** Male C57BL/6 wild-type (WT) mice, aged six to eight weeks (n = 110, n = 6 per group, randomly grouped), together with DOCK2-deficient (DOCK2-KO) mice (n = 6), were housed under standard laboratory conditions. SCIRI model was induced by transient occlusion of the abdominal aorta, following a previously reported method with slight modifications (Rong *et al.*, 2022). Briefly, mice were anesthetized with 2-3% isoflurane inhalation, maintained at 36.5-37.5°C using a temperature-controlled heating pad during surgery, and received subcutaneous injection of buprenorphine (0.1 mg/kg) for analgesia and 1 mL normal saline for hydration post-operatively. Specifically, the vessel was clamped for 60 minutes just below the left renal artery using a microvascular clip, after which circulation was restored by removing the clip. Sham animals received identical laparotomy without aortic occlusion. Spinal cord samples were harvested at different points in time following reperfusion (early reperfusion phase: 3 h and 6 h; peak neuronal damage phase: 12 h and 24 h; persistent injury-to-repair transition: 36 h; active repair phase: 48 h and72 h; late repair/stabilization phase: 96 h) for further analyses. Motor function was assessed with the Basso Mouse Scale (BMS, 0-9 points) at 0, 6, 12, 24, 48, and 72 h after SCIRI. All animal experiments were approved by the Institutional Animal Care and Use Committee of the China Medical University (CMUKT2024182).

**HE staining:** The paraformaldehyde-fixed spinal cord tissues were exposed to the standard HE staining procedure (Beyotime Institute of Biotechnology) (Zhang *et al.*, 2025). Pathological changes (e.g., neuronal necrosis, inflammatory cell infiltration, and tissue edema) were observed under a light microscope.

**Immunofluorescence:** Paraffin-embedded spinal cord sections underwent standard immunofluorescent staining procedure (Zhang *et al.*, 2025). The primary antibodies included anti-MAP2 (1:500; Abcam, ab5392), anti-NeuN (1:500; Abcam, ab177487), and anti-DOCK2 (1:200; Abcam, ab204372). Corresponding fluorochrome-conjugated secondary antibodies (Alexa Fluor 488-conjugated goat anti-mouse IgG, 1:1000; Thermo Fisher Scientific, A11001; Alexa Fluor 594-conjugated goat anti-rabbit IgG, 1:1000; Thermo Fisher Scientific, A11012) were incubated at room temperature for 1 h in the dark to avoid fluorochrome quenching.

**Primary Spinal Cord Neuron Isolation and Culture:** Primary spinal cord neurons were obtained from C57BL/6 mouse embryos at embryonic day 16 (E16) according to previous reports (Agalave *et al.*, 2020). To confirm neuronal identity, immunofluorescence staining was carried out using the neuronal marker microtubule-associated protein 2 (MAP2).

**OGD/R treatment, Adenovirus Infection and Rapamycin incubation**

**OGD/R treatment:** The isolated primary neurons were washed twice with glucose-free DMEM/F12 and incubated in glucose-free DMEM in a hypoxic chamber (95% $N_2$ and 5% $CO_2$, gas flow rate: 8 L/min). After OGD for 1 h (hypoxic duration), the neurons were transferred to a normoxic incubator maintained at 37°C in a humidified incubator containing 5% $CO_2$ for 2 h (reoxygenation duration) before subsequent assays.

**Adenovirus Infection:** Short hairpin RNA (shRNA) targeting mouse DOCK2 (AV-shDOCK2) and negative control shRNA (AV-shNC) were constructed and packaged in adenovirus vector (Hunan Fenghui Biotechnology Co., Ltd.). Primary neurons were infected with adenoviruses ($1 \times 10^9$ PFU/mL). After 24 h of infection, cells were collected to verify infection efficiency via real time PCR and western blotting targeting DOCK2.

**Rapamycin incubation:** Primary neurons were transduced with AV-shDOCK2 for 24 h, followed by oxygen-glucose deprivation/reperfusion (OGD/R) exposure. During this process, Rapamycin (0.5 μM), an autophagy activator, was applied simultaneously for an additional 24 h (Cheng *et al.*, 2021).

**Ferroptosis induction:** After 24 h of AV-shDOCK2 infection, neurons were exposed to OGD/R while being treated with the ferroptosis inducer erastin (5 μM, MCE) (Li *et al.*, 2023).

**CCK-8:** Cell viability was assessed with the CCK-8 assay kit (Hu *et al.*, 2021), and absorbance at 450 nm was recorded using a Bio-Rad microplate reader.

**GSH-Px, MDA and iron level detection:** GSH-Px activity, MDA levels and intracellular $Fe^{2+}$ concentrations measured using corresponding commercial kits (Nanjing Jiancheng Bioengineering Institute).

**Sevoflurane Preconditioning in SCIRI Mice:** Three days before sevoflurane preconditioning, the mice were intrathecally injected with DOCK2 overexpression adenovirus (AV-DOCK2; $5\times10^8$ PFU/mL, 5 μL) or empty vector (AV-vector) between the L5–L6 vertebrae. Mice were placed in a sealed chamber and exposed to a gas mixture of 33% $O_2$, 2.4% sevoflurane for 1 h. Then, the mice were subjected to SCIRI operation. Motor function was evaluated using the BMS scoring system and spinal cord tissues were collected to detect the occurrence of ferroptosis.

**Western blotting:** The Western blot procedures were performed as previously described (Zhang *et al.*, 2025). The primary antibodies included: anti-DOCK2 (1:1000, Abcam, Cat. No.: ab204372), anti-LC3B (1:1000, Abcam, Cat. No.: 192890), anti-p62 (1:1000, Abcam, Cat. No.: 109012), anti-Atg5 (1:1000, Abcam, Cat. No.: 108327), anti-p-mTOR (Ser2448, 1:1000, Abcam, Cat. No.: 109268), anti-mTOR (1:1000, Abcam, Cat. No.: 134903) and anti-GAPDH (1:5000, Abcam, Cat. No.: ab9485) as the loading control for protein normalization.

**Real-time PCR:** Real-time PCR was conducted with SYBR Premix Ex Taq ™ II (TaKaRa) on an Exicycler ™ 96 platform (Bioneer). DOCK2 mRNA expression was quantified by the $2^{-\Delta\Delta Ct}$ method. The primer sequences were as follows: DOCK2 forward, 5'-CGAGGAAGTAGTGAAGTT-3'; reverse, 5'-TGAGTGGCGACTTTCAT-3' (Zhang *et al.*, 2025).

**Statistical Analysis:** Data are shown as mean ± standard deviation. Statistical analyses were performed using GraphPad Prism software 8.0. Statistical analyses were conducted with one-way ANOVA followed by Tukey's test, or Student's t-test. $P<0.05$ was considered statistically significant.

## RESULTS

**DOCK2 is upregulated in spinal cord tissues of SCIRI mice and OGD/R-treated primary spinal neurons:** To investigate the effects of DOCK2 on SCIRI, a model of SCIRI was established in mice by clamping the abdominal aorta. The BMS score indicated that the SCIRI mice showed motor function impairment (Fig. 1A, $P<0.05$). As shown in Fig. 1B and C, the mRNA level of DOCK2 was significantly increased at 3 h post SCIRI, peaked at 24 h with a significant 6-fold increase, and its protein level peaked at 24 h with a significant 4-fold increase, then gradually decreased from 36 h to 96 h. HE staining revealed severe pathological damage in the spinal cord of SCIRI mice at 24 h post-injury, whereas the Sham group showed normal spinal cord morphology (Fig. 1D). Immunofluorescence double staining with NeuN and DOCK2 revealed colocalization, suggesting that DOCK2 is predominantly expressed in neurons following SCIRI (Fig. 1E). To further validate its expression pattern in vitro, primary spinal neurons were isolated and confirmed by MAP2 staining, which showed strong positivity (Fig. 1F). These neurons were subsequently exposed to OGD/R. Real-time PCR and Western blot analyses demonstrated that OGD/R markedly elevated DOCK2 mRNA and protein expression compared with controls (Fig. 1G, $P<0.05$). Collectively, these findings indicate that DOCK2 is upregulated in both SCIRI mouse spinal cord tissues and OGD/R-challenged primary spinal neurons.

**DOCK2 depletion inhibits OGD/R-induced ferroptosis in primary spinal neurons:** To investigate the role of DOCK2, AV-shDOCK2 was generated and introduced into primary spinal neurons. Real-time PCR and western blotting demonstrated that DOCK2 expression at both mRNA and protein levels was markedly reduced following AV-shDOCK2 transfection compared with controls (Fig. 2A, 2B, $P<0.05$). Moreover, CCK-8 analysis revealed that OGD/R challenge caused a significant decline in neuronal viability, whereas DOCK2 knockdown markedly improved cell survival (Fig. 2C, $P<0.05$).

Interestingly, we found that the restoration of neuronal viability by DOCK2 depletion was abolished by the ferroptosis inducer erastin (Fig. 2D, $P<0.05$)., confirming that DOCK2's effect is mediated through the ferroptosis pathway. Biochemical assays showed that OGD/R treatment significantly decreased GSH-Px activity and increased MDA level and $Fe^{2+}$ content compared with the control neurons, which could be reversed by DOCK2 depletion (Fig. 2E-G, $P<0.05$). The data indicated that DOCK2 depletion conferred a protective effect against OGD/R-induced ferroptosis in spinal cord neurons.

**DOCK2 mediates OGD/R-induced neuronal ferroptosis through regulating autophagy:** Autophagy and ferroptosis are intimately linked regulatory processes. To determine whether DOCK2 affects ferroptosis via autophagy, the primary neurons transfected with AV-

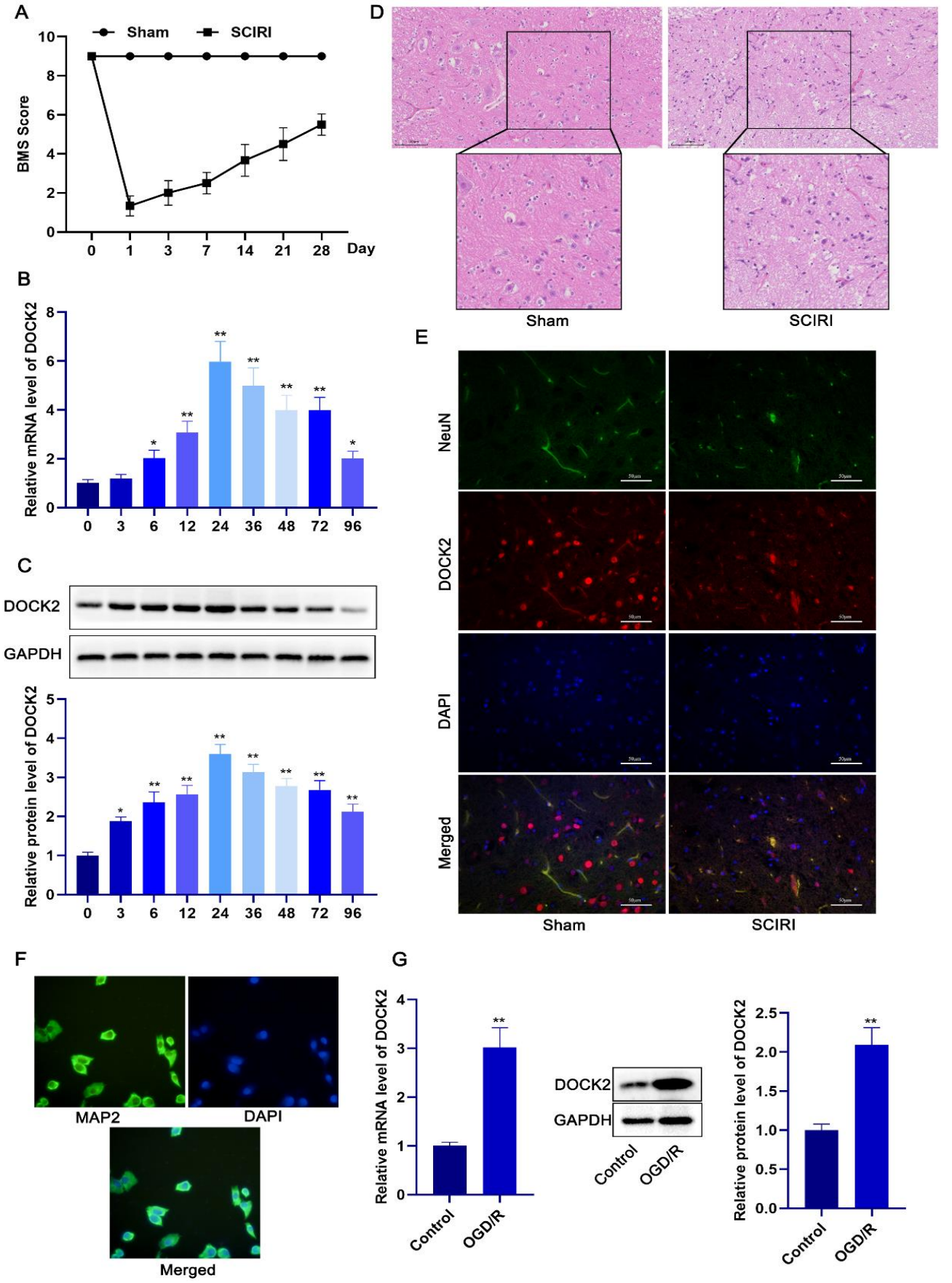


**Fig. 1:** DOCK2 is upregulated in spinal cord tissues of SCIRI mice and OGD/R-treated primary spinal neurons. (A) BMS scores assessing motor function in Sham and SCIRI mice over time (B) DOCK2 mRNA expression levels in spinal cord tissues at various time points post-SCIRI (C) Western blot analysis of DOCK2 protein expression in spinal cord tissues post-SCIRI (D) HE staining showing pathological changes in the spinal cord at 24 h post-SCIRI. (E) Immunofluorescence colocalization of DOCK2 (red) and the neuronal marker NeuN (green) in spinal cord sections. (F) Identification of primary spinal neurons by MAP2 immunofluorescence staining. (G) DOCK2 mRNA and protein levels in primary neurons after OGD/R treatment. Data are represented as mean ± SD (n=6) and are analyzed by one-way ANOVA or unpaired t test. *P<0.05, **P<0.01 vs. Sham group.

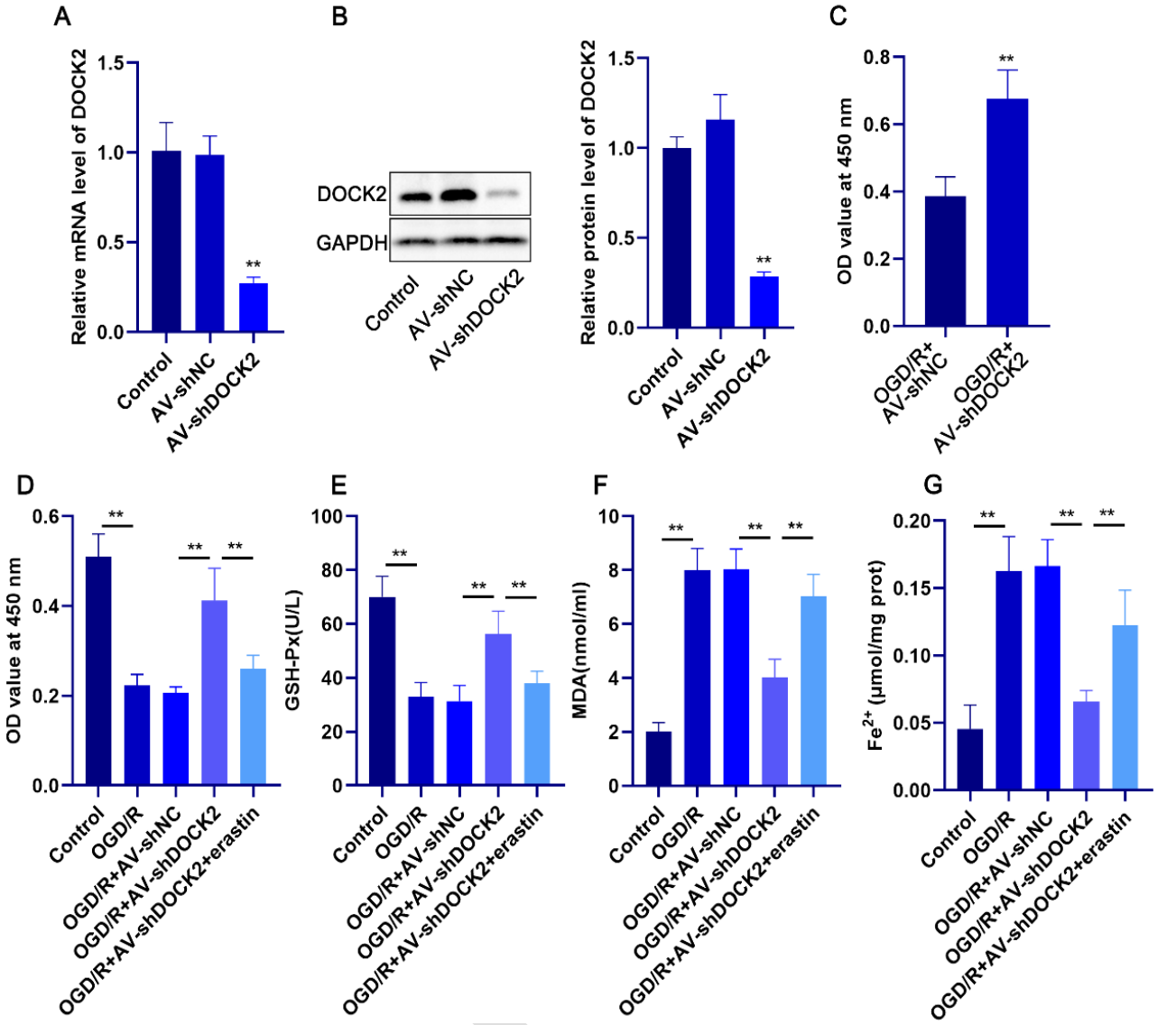


**Fig.2:** DOCK2 depletion inhibits OGD/R-induced ferroptosis in primary spinal neurons. (A, B) DOCK2 mRNA and protein levels after transfection with AV-shDOCK2 (C) CCK-8 assay showing neuronal viability after OGD/R with or without DOCK2 depletion. (D) Effect of the ferroptosis inducer erastin on DOCK2 depletion-mediated neuroprotection. (E-G) Biochemical analysis of GSH-Px activity, MDA levels and $Fe^{2+}$ content under different treatment conditions. Data are represented as mean ± SD and are analyzed by one-way ANOVA test. *P<0.05, **P<0.01 vs. the AV-shNC group or indicated group.

shDOCK2 were treated with OGD/R combined with autophagy activator rapamycin. Western blot analysis (Fig. 3A) demonstrated that DOCK2 depletion significantly decreased autophagic activity, as evidenced by a reduction in the LC3-II/p62 ratio compared to OGD/R-treated controls (P<0.05); conversely, rapamycin treatment re-activated autophagy in DOCK2-depleted neurons, restoring the LC3-II/p62 ratio (P<0.05). Biochemical assays showed that rapamycin treatment also reversed the protective effect of DOCK2 depletion on ferroptosis, manifested as the changes in iron accumulation, GSH-Px activity and MDA content (Fig. 3B-D, P＜0.05), indicating that DOCK2 mediates OGD/R-induced neuronal ferroptosis by regulating autophagy.

**DOCK2 knockout alleviates autophagy-associated ferroptosis in SCIRI mice:** To validate the in vivo function of DOCK2, SCIRI models were generated using DOCK2-KO mice. Real-time PCR and western blotting demonstrated that DOCK2 expression at both mRNA and protein levels was absent in DOCK2-KO mice, whereas SCIRI markedly upregulated DOCK2 in WT counterparts (Fig. 4A–B, P<0.05). SCIRI mice had the lowest BMS score, while DOCK2-KO+SCIRI mice had a significantly higher BMS score than SCIRI mice (Fig. 4C, P＜0.05). Immunohistochemical staining of ChAT, a motor neuron marker, showed that SCIRI significantly reduced ChAT-positive neurons and DOCK2 knockout increased ChAT-positive neurons (Fig. 4D). Similarly, SCIRI-induced spinal cord pathological damage alleviated in DOCK2-KO mice (Fig. 4E). Meanwhile, SCIRI significantly increased the expression of LC3B-II/I and Atg5 protein level, and decreased p62 protein, while DOCK2 knockout reversed these changes in the spinal tissues (Fig. 4F, P＜0.05). DOCK2 knockout significantly increased GSH-Px activity and decreased MDA level and $Fe^{2+}$ content in the spinal cord (Fig. 4G, P＜0.05). The data suggested that DOCK2 depletion alleviates autophagy-associated ferroptosis in vivo.

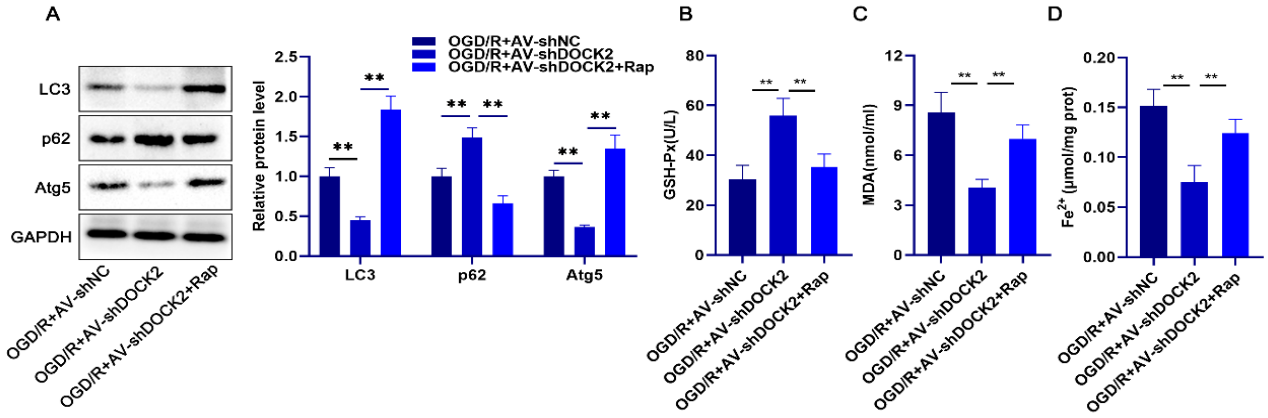


**Fig.3:** DOCK2 mediates OGD/R-induced neuronal ferroptosis through regulating autophagy. (A) Western blot analysis of autophagy markers (LC3, p62 and Atg5) after rapamycin treatment. (B-D) Effects of rapamycin on $Fe^{2+}$ content, GSH-Px activity, and MDA levels in OGD/R-treated neurons with DOCK2 depletion. Data are represented as mean ± SD and are analyzed by one-way ANOVA test. *P<0.05, **P<0.01 vs. the indicated group.

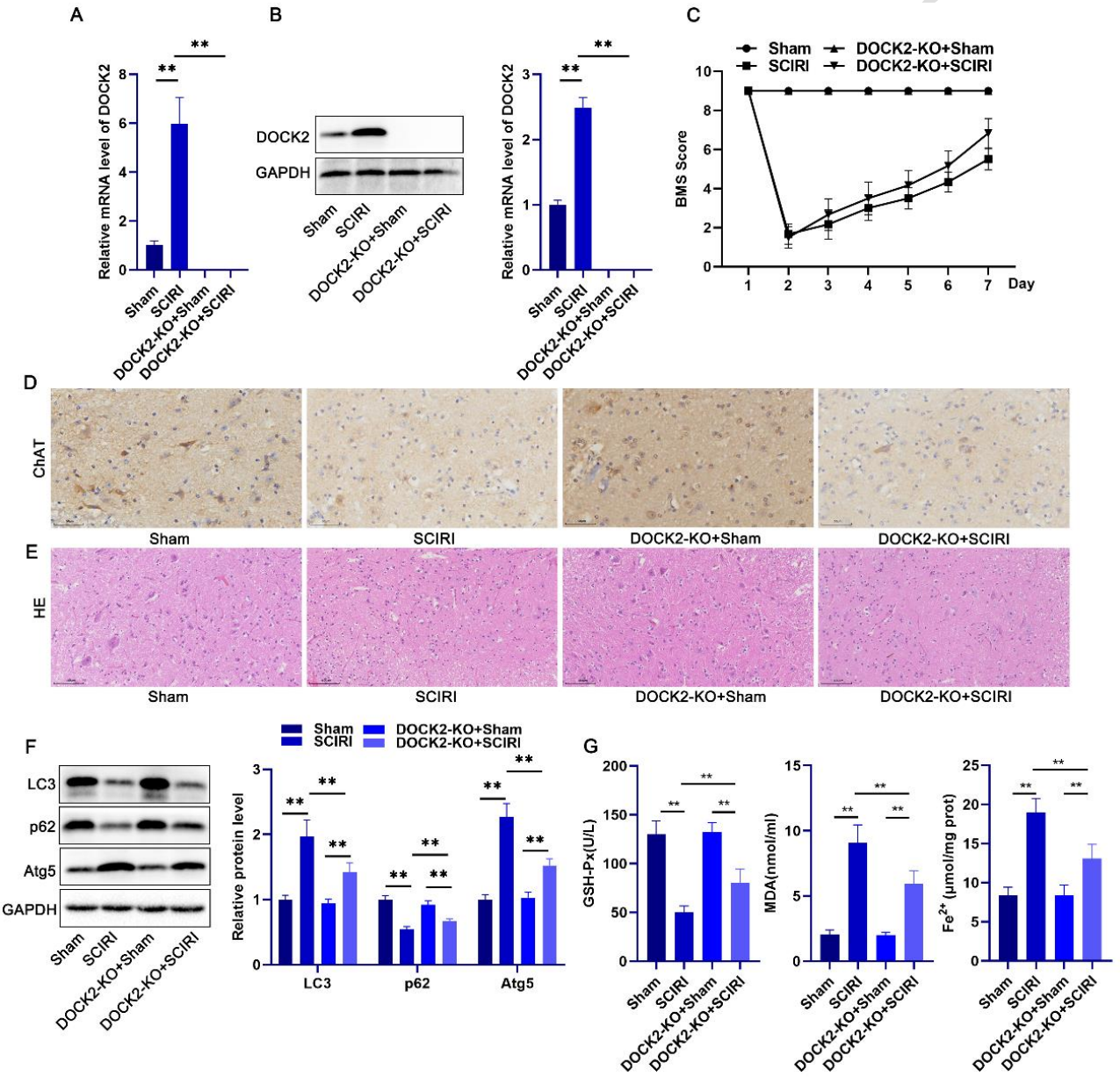


**Fig.4:** DOCK2 knockout alleviates autophagy-associated ferroptosis in SCIRI mice. **(**A, B) DOCK2 mRNA and protein expression in WT and DOCK2-KO mice. (C) BMS scores showing motor function recovery in DOCK2-KO mice after SCIRI. (D) immunohistochemical staining targeting ChAT in spinal cord tissues post-SCIRI. (E) HE staining showing pathological changes in the spinal cord tissue of DOCK2-KO mice after at 24 h post-SCIRI. (F) Western blot analysis of autophagy markers (LC3, p62 and Atg5) in spinal cord tissues. (G) Biochemical analysis of GSH-Px activity, MDA levels, and $Fe^{2+}$ content in spinal cord tissues (P<0.05). Data are represented as mean ± SD (n = 6) and are analyzed by one-way ANOVA test. *P<0.05, **P<0.01 vs. the indicated group.

**DOCK2 mediates the protective effect of sevoflurane pretreatment against SCIRI:** To examine the role of DOCK2 in sevoflurane-mediated protection against SCIRI, mice received intrathecal AV-DOCK2 injection for 3 days before sevoflurane pretreatment and SCIRI induction. As illustrated in Fig. 5A, sevoflurane markedly improved motor function in SCIRI mice, whereas DOCK2 overexpression abolished this benefit ($P<0.05$). Moreover, sevoflurane pretreatment reduced LC3B-II/Atg5 expression and elevated p62 levels compared with the SCIRI group, effects that were reversed by DOCK2 overexpression (Fig. 5B, $P<0.05$). Comparable trends were observed for GSH, MDA, and $Fe^{2+}$ levels (Fig. 5C, $P<0.05$). Collectively, these findings suggest that DOCK2 mediates the protective effects of sevoflurane pretreatment in SCIRI.

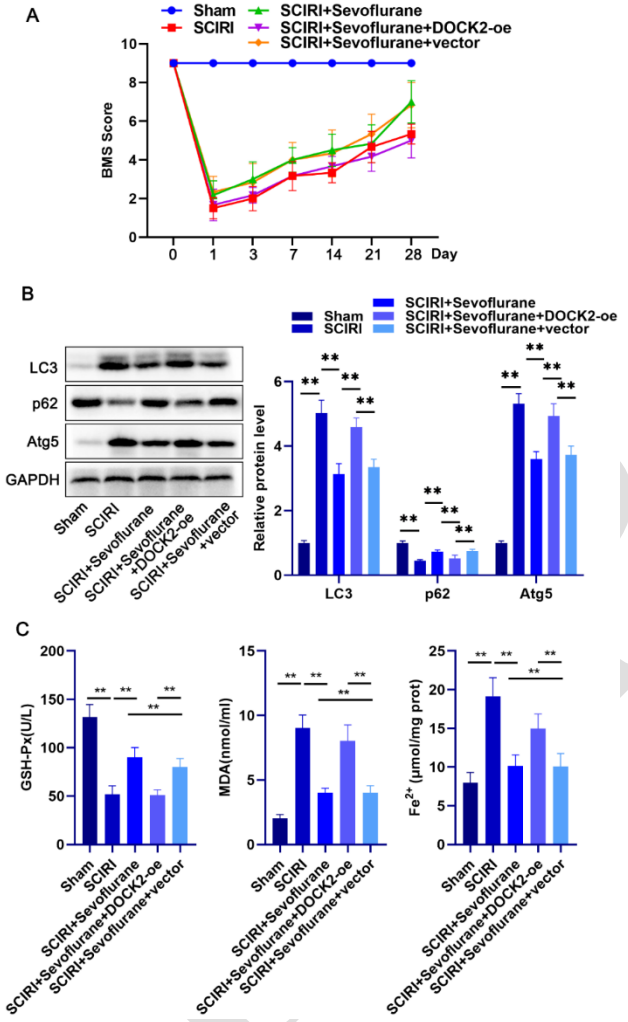


**Fig.5:** DOCK2 mediates the protective effect of sevoflurane pretreatment against SCIRI. (A) BMS scores in sevoflurane pretreatment mice exposed to SCIRI. (B) Western blot analysis showing that sevoflurane modulates autophagy marker (LC3, p62 and Atg5) expression in the spinal cord tissue of mice with SCIRI treatment. (C) Biochemical analysis of GSH-Px activity, MDA levels, and $Fe^{2+}$ content in spinal cord tissues of mice with SCIRI treatment. Data are represented as mean ± SD (n = 6) and are analyzed by one-way ANOVA test. *P < 0.05, **P < 0.01 vs. the indicated group.

## DISCUSSION

SCIRI poses a significant clinical burden in veterinary practice, particularly in companion animals and livestock (Fuentealba *et al.*, 1991; Sebastian and Giles, 2004). However, the current supportive therapies often fail to address the core pathological cascades of SCIRI, underscoring the necessity to elucidate species-specific mechanistic pathways for targeted intervention. Our study addressed this gap by investigating DOCK in SCIRI in mice, a usual veterinary-relevant model. In murine SCIRI, DOCK2 mRNA and protein levels were increased and peaked at 24 h post-reperfusion, accompanied by severe motor dysfunction. Critically, genetic ablation of DOCK2 resulted in enhanced locomotor function and increased survival of choline acetyltransferase (ChAT)-positive motor neurons in mice. Besides, the depletion of DOCK2 inhibit excessive autophagy in vivo murine SCIRI models and in vitro primary spinal cord neuron OGD/R models, and ultimately involves in iron-dependent ferroptosis suppression.

It is well understood that neuroinflammation-mediated secondary injury is a critical mechanism contributing to neurological damage in SCIRI (Anwar *et al.*, 2016; Krause *et al.*, 2022). This cascade is initiated within minutes after ischemic onset and may persist for weeks, sustained by ongoing microglial activation, peripheral immune cell infiltration, and excessive release of inflammatory mediators including TNF-α and IL-1β (Kahveci *et al.*, 2021). Concurrent oxidative stress and mitochondrial dysfunction further amplify neural cell apoptosis and white matter degeneration, ultimately leading to severe and often irreversible motor deficits (Xie *et al.*, 2023). Accordingly, modulation of secondary injury mechanisms has emerged as a pivotal therapeutic approach to attenuate SCIRI-related neurological deficits and enhance functional recovery. Growing evidence indicates that DOCK2 acts as a key regulator in multiple cellular activities. As a member of the cytoskeletal regulatory protein family, DOCK2 serves as an important guanine nucleotide exchange factor (GEF), specifically promoting the activation of Rac1 and Rac2 through GDP-GTP exchange. (Qiu *et al.*, 2025; Zhou and Hu, 2022). Recently, DOCK2 is increasingly recognized for its functional significance in the pathogenesis of neurological disorders. Notably, DOCK2 modulates primary immune functions in microglial cells, including cytokine release, phagocytic activity, and paracrine-mediated neurotoxicity (Cimino *et al.*, 2009). Meanwhile, Yu *et al.* have reported that DOCK2 plays the promoting effects on microglia activation and DOCK2 knockdown inhibited neuroinflammation and attach neuroprotection post spinal cord injury in rodents (Zhang *et al.*, 2025). In the current study, we found that DOCK2 was specifically localized in neurons. Besides, DOCK2 was highly expressed after SCIRI treatment in vivo as well as OGD/R in vitro. Hence, we deduce DOCK2 deficiency maybe beneficial for SCIRI. Notably, prior veterinary research on DOCK2 focused on infectious diseases (Li *et al.*, 2021), but our data extend its relevance to neurological injury, positioning it as a target to concurrently reduce nerve injury after SCIRI.

Classical pathways including neuroinflammation and oxidative stress are recognized as drivers of SCIRI in animals, while emerging evidence highlights the critical role of the functional interaction between two evolutionarily conserved cellular processes—autophagy and ferroptosis (Hou *et al.*, 2016; Xiong *et al.*, 2020; Yan

*et al.*, 2025). Our data showed that DOCK2 silencing in neurons with OGD/R treatment reduced autophagic flux dysregulation and mitigated ferroptosis. Importantly, rapamycin-induced autophagy reversal abolished these protections, confirming that autophagy-dependent ferroptosis constitutes a key pathway mediated by DOCK2. Moreover, these molecular insights hold significant translational potential for veterinary medicine and DOCK2 may represent a promising therapeutic target for mitigating SCIRI in companion animals and livestock. Extensive research has well-established the protective effect of sevoflurane, a commonly used inhalational anesthetic in veterinary medicine, against SCIRI (Wang *et al.*, 2021), the mechanisms by which confers this protection are still poorly understood and require further investigation. Additionally, we investigated whether DOCK2 mediates the protective effects of sevoflurane, against SCIRI. These data in our work suggest that sevoflurane preconditioning alleviates SCIRI by inhibiting DOCK2 partly, providing new evidence for its utility in veterinary anesthesia and perioperative care. Despite the novel insights gained, this study has several limitations that warrant consideration. These findings are primarily derived from murine models, and species-specific differences in DOCK2 expression patterns, autophagy-ferroptosis crosstalk, and SCIRI pathophysiology may exist between mice and veterinary-relevant species (e.g., dogs, cats, livestock), which requires validation in large animal models closer to clinical veterinary practice.

In conclusion, our study establishes DOCK2 as a critical therapeutic target in SCIRI via inhibiting autophagy-dependent ferroptosis and sevoflurane preconditioning represents a safe and clinically feasible strategy to mitigate SCIRI in spinal surgery animals, with DOCK2 serving as a key mediator.

## REFERENCES


Agalave, N.M., Lane, B.T., Mody, P.H., *et al.*, 2020. Isolation, culture, and downstream characterization of primary microglia and astrocytes from adult rodent brain and spinal cord. J Neurosci Methods 340: 108742.

Anwar, M.A., Al Shehabi, T.S., Eid, A.H., 2016. Inflammogenesis of Secondary Spinal Cord Injury. Front Cell Neurosci 10: 98.

Awad, H., Efanov, A., Rajan, J., *et al.*, 2021. Histological Findings After Aortic Cross-Clamping in Preclinical Animal Models. J Neuropathol Exp Neurol 80: 895-911.

Azari, O., Kheirandish, R., Azizi, S., *et al.*, 2015. Protective Effects of Hydrocortisone, Vitamin C and E Alone or in Combination against Renal Ischemia-Reperfusion Injury in Rat. Iran J Pathol 10: 272-280.

Bell, M.T., Puskas, F., Smith, P.D., *et al.*, 2012. Attenuation of spinal cord ischemia-reperfusion injury by specific α-2a receptor activation with dexmedetomidine. J Vasc Surg 56: 1398-1402.

Borgens, R.B., Liu-Snyder, P., 2012. Understanding secondary injury. Q Rev Biol 87: 89-127.

Chen, X., Yu, C., Kang, R., *et al.*, 2021. Cellular degradation systems in ferroptosis. Cell Death Differ 28: 1135-1148.

Cheng, J.T., Liu, P.F., Yang, H.C., *et al.*, 2021. Tumor Susceptibility Gene 101 facilitates rapamycin-induced autophagic flux in neuron cells. Biomed Pharmacother 134: 111106.

Cimino, P.J., Sokal, I., Leverenz, J., *et al.*, 2009. DOCK2 is a microglial specific regulator of central nervous system innate immunity found in normal and Alzheimer's disease brain. Am J Pathol 175: 1622-1630.

Cimino, P.J., Yang, Y., Li, X., *et al.*, 2013. Ablation of the microglial protein DOCK2 reduces amyloid burden in a mouse model of Alzheimer's disease. Exp Mol Pathol 94: 366-371.

Ding, S., Cao, Y., Lu, X., *et al.*, 2022. Dedicator of Cytokinesis 2 (DOCK2) Silencing Protects Against Cerebral Ischemia/Reperfusion by Modulating Microglia Polarization via the Activation of the STAT6 Signaling Pathway. Neuroscience 491: 110-121.

Eryilmaz, F., Farooque, U., 2021. The Efficacy of Combined Medication With Methylprednisolone and Erythropoietin in the Treatment of Ischemia-Reperfusion Injury to the Spinal Cord in Patients With Cervical Spondylotic Myelopathy. Cureus 13: e14018.

Fuentealba, I.C., Weeks, B.R., Martin, M.T., *et al.*, 1991. Spinal cord ischemic necrosis due to fibrocartilaginous embolism in a horse. J Vet Diagn Invest 3: 176-179.

Guo, X., Chen, S.Y., 2017. Dedicator of Cytokinesis 2 in Cell Signaling Regulation and Disease Development. J Cell Physiol 232: 1931-1940.

Hafezi, B., Kazemi Mehrjerdi, H., Moghaddam Jafari, A., 2024. Effect of captopril on paraplegia caused by spinal cord ischemia-reperfusion injury in rats. Vet Res Forum 15: 379-385.

Hou, W., Xie, Y., Song, X., *et al.*, 2016. Autophagy promotes ferroptosis by degradation of ferritin. Autophagy 12: 1425-1428.

Hu, J., Yu, Q., Xie, L., *et al.*, 2016. Targeting the blood-spinal cord barrier: A therapeutic approach to spinal cord protection against ischemia-reperfusion injury. Life Sci 158: 1-6.

Hu, Z., Yuan, Y., Zhang, X., *et al.*, 2021. Human Umbilical Cord Mesenchymal Stem Cell-Derived Exosomes Attenuate Oxygen-Glucose Deprivation/Reperfusion-Induced Microglial Pyroptosis by Promoting FOXO3a-Dependent Mitophagy. Oxid Med Cell Longev 2021: 6219715.

Ji, L., Xu, S., Luo, H., Zeng, F., 2022. Insights from DOCK2 in cell function and pathophysiology. Front Mol Biosci 9: 997659.

Kahveci, F.O., Kahveci, R., Gokce, E.C., *et al.*, 2021. Biochemical, pathological and ultrastructural investigation of whether lamotrigine has neuroprotective efficacy against spinal cord ischemia reperfusion injury. Injury 52: 2803-2812.

Krause, J.S., Cao, Y., DiPiro, N.D., 2022. The Relationship of Secondary and Chronic Health Conditions With Emergency Department Visits and Related Hospitalizations Among People With Traumatic Spinal Cord Injury. Arch Phys Med Rehabil 103: 2338-2344.

Li, D., Lu, X., Xu, G., *et al.*, 2023. Dihydroorotate dehydrogenase regulates ferroptosis in neurons after spinal cord injury via the P53-ALOX15 signaling pathway. CNS Neurosci Ther 29: 1923-1939.

Li, W., Li, J., He, N., *et al.*, 2021. Molecular mechanism of enhancing the immune effect of the Newcastle disease virus vaccine in broilers fed with Bacillus cereus PAS38. Food Funct 12: 10903-10916.

Lin, S., Xu, C., Lin, J., *et al.*., 2021. Regulation of inflammatory cytokines for spinal cord injury recovery. Histol Histopathol 36: 137-142.

Liu, S., Yao, S., Yang, H., *et al.*, 2023. Autophagy: Regulator of cell death. Cell Death Dis 14: 648.

Luo, C., Tao, L., 2020. The Function and Mechanisms of Autophagy in Spinal Cord Injury. Adv Exp Med Biol 1207: 649-654.

Mizushima, N., Komatsu, M., 2011. Autophagy: renovation of cells and tissues. Cell 147: 728-741.

Qiu, J., Qu, Y., Li, Y., *et al.*, 2025. Inhibition of RAC1 activator DOCK2 ameliorates cholestatic liver injury via regulating macrophage polarisation and hepatic stellate cell activation. Biol Direct 20: 21.

Rong, Y., Fan, J., Ji, C., *et al.*., 2022. USP11 regulates autophagy-dependent ferroptosis after spinal cord ischemia-reperfusion injury by deubiquitinating Beclin 1. Cell Death Differ 29: 1164-1175.

Sabzvar, M.K., Cho, E.B., Yuan, X., *et al.*, 2025. An inhibitor of UHM splicing factors exerts anti-leukemic activity by altering cell cycle progression and reducing lysosome acidification. Cell Signal 136: 112112.

Sebastian, M.M., Giles, R.C., 2004. Fibrocartilaginous embolic myelopathy in a horse. J Vet Med A Physiol Pathol Clin Med 51: 341-343.

Shi, Z., Yuan, S., Shi, L., *et al.*, 2021. Programmed cell death in spinal cord injury pathogenesis and therapy. Cell Prolif 54: e12992.

Simon, F., Floros, N., Ibing, W., *et al.*, A., 2019. Neurotherapeutic potential of erythropoietin after ischemic injury of the central nervous system. Neural Regen Res 14: 1309-1312.

Stockwell, B.R., Jiang, X., Gu, W., 2020. Emerging Mechanisms and Disease Relevance of Ferroptosis. Trends Cell Biol 30: 478-490.

Wang, D., Fang, B., Wang, Z., *et al.*, 2021. Sevoflurane pretreatment regulates abnormal expression of MicroRNAs associated with spinal cord ischemia/reperfusion injury in rats. Ann Transl Med 9: 752.

Wang, Y.C., Zhang, S., Du, T.Y., *et al.*, 2010. Hyperbaric oxygen preconditioning reduces ischemia-reperfusion injury by stimulating autophagy in neurocyte. Brain Res 1323: 149-151.

Xie, L., Wu, H., Huang, X., *et al.*, 2023. Melatonin, a natural antioxidant therapy in spinal cord injury. Front Cell Dev Biol 11: 1218553.

Xing, Y., Xiao, Y.Z., Zhao, M., *et al.*, 2025. The role of oxidative stress in spinal cord ischemia reperfusion injury: mechanisms and therapeutic implications. Front Cell Neurosci 19: 1590493.

Xiong, Y., Xia, Y., Deng, J., *et al.*, 2020. Direct Peritoneal Resuscitation with Pyruvate Protects the Spinal Cord and Induces Autophagy via

Regulating PHD2 in a Rat Model of Spinal Cord Ischemia-Reperfusion Injury. Oxid Med Cell Longev 2020: 4909103.

Xu, Z., Li, Z., 2020. Experimental Study on the Role of Apelin-13 in Alleviating Spinal Cord Ischemia Reperfusion Injury Through Suppressing Autophagy. Drug Des Devel Ther 14: 1571-1581.

Yan, L., Feng, Q., Sun, Y., *et al.*, 2025. Selenized Tripterine Phytosomes Alleviate Ferroptosis-Mediated Acute Kidney Injury by Suppressing GPX4 Degradation via the DUSP1/Autophagy Pathway. Biomater Res 29: 0236.

Yao, X., Zhang, Y., Hao, J., *et al.*, 2019. Deferoxamine promotes recovery of traumatic spinal cord injury by inhibiting ferroptosis. Neural Regen Res 14: 532-541.

Yin, J., Yin, Z., Wang, B., *et al.*, 2019. Angiopoietin-1 Protects Spinal Cord Ischemia and Reperfusion Injury by Inhibiting Autophagy in Rats. Neurochem Res 44: 2746-2754.

Zhang, H., Xiang, L., Yuan, H., *et al.*, 2025. DOCK2 deficiency alleviates neuroinflammation and affords neuroprotection after spinal cord injury. Biochim Biophys Acta Mol Cell Res 1872: 119882.

Zheng, Q., Wang, D., Lin, R., *et al.*, 2025. Pyroptosis, ferroptosis, and autophagy in spinal cord injury: regulatory mechanisms and therapeutic targets. Neural Regen Res 20: 2787-2806.

Zhou, B., Liu, J., Kang, R., *et al.*, 2020. Ferroptosis is a type of autophagy-dependent cell death. Semin Cancer Biol 66: 89-100.

Zhou, K., Sansur, C.A., Xu, H., *et al.*, The Temporal Pattern, Flux, and Function of Autophagy in Spinal Cord Injury. Int J Mol Sci 18.

Zhou, Y., Hu, W., 2022. Dedicator of cytokinesis protein 2 knockdown ameliorates LPS-induced acute lung injury by modulating Rac1/2 activity. Allergol Immunopathol (Madr) 50: 38-46.

Zhu, Y., Zhang, J., Deng, Q. *et al.*, 2024. Mitophagy-associated programmed neuronal death and neuroinflammation. Front Immunol 15: 1460286.